

Why does ITD Sensitivity Break Down in Electric Hearing? A Modeling Study

Werner Hemmert¹, Albert Croner¹, Jörg Encke², Siwei Bai¹

¹ *Bio-inspired Information Processing, Munich Institute of Biomedical Engineering,
Technical University of Munich, 85748 Garching*

² *Medical Physics and Acoustics, Carl von Ossietzky University of Oldenburg, 26111 Oldenburg, Germany*

Introduction

With more than 1 million implanted devices, cochlear implants (CIs) are the most successful neuroprostheses. They bring back hearing to adults with severe to complete hearing loss and they enable newborns with hereditary hearing disorders to hear sounds and learn spoken language(s). CI users usually achieve open speech understanding, which allows them to communicate and to be part of our society. Most children with CIs attend regular schools. Despite this progress, CI users still lack behind normal hearing subjects especially in noisy and reverberant environments and in cocktail party scenarios, where normal hearing subjects can localize sound sources and focus on one speaker. Sound localization and suppression of noise and reverberation relies crucially on the processing of the temporal fine-structure. However, CI coding strategies cannot (or only to a very limited extent) convey high-resolution temporal fine-structure information, mostly because of the broad current spread along the cochlea, which leads to severe cross talk between frequency channels [1]. But even under laboratory conditions, where pulse trains with a precisely defined temporal shift between bilateral CI users are delivered to single CI electrodes, sensitivity to interaural time differences (ITD) in CI users is at least one order of magnitude worse than in normal hearing subjects [2]. This is surprising, as synchronization of action potentials in single auditory nerve fibers to electrical stimulation has been described as even sharper than in normal hearing [3].

We therefore analyze the temporal properties of electrically evoked responses with our detailed model, which is based on an anatomical precise human cochlea and multi-compartment models and we consider different degeneration states of the spiral ganglion neurons.

Methods

We have previously developed a model of the cochlea based on high-resolution micro-computed tomography of a human cadaveric temporal bone with a voxel size of $5.9 \mu\text{m}$ [4]. To fit the model into the memory of our computer, the images were cropped to include only the cochlea and its immediate surroundings and later downsampled to an isotropic resolution of $9.6 \mu\text{m}$ with a spatial resolution of $930 \times 930 \times 1,014$ voxels. The bony structures were carefully segmented, especially the porous modiolus. Then compartments consisting of bone and containing cochlear fluids were defined and a surface triangular mesh was generated. A special compartment was defined within the pores of the modiolus, in which the auditory nerve is embedded. Therefore, the pores in the modiolus define the path of the auditory nerve fibers, the spiral ganglion neurons (SGN).

They are resolved well enough in our scan to show where their cell bodies are located in Rosenthal's channel and how their dendrites branch in the direction of the inner hair cells in the osseus spiral lamina (OSL).

We used a model-based algorithm to reconstruct the path of single nerve fibers. We defined the start points for 400 fibers at the edge of the OSL equally distributed along the length of the cochlea and their end points at the end of the inner ear canal, which is close to the target of the nerve in the brainstem. We also included a 45° rotation, which replicates the twist of the fibers in the auditory nerve. From the reconstruction one can see how the dendrites form bundles in the OSL and how their axons run along the central hole in the modiolus.

A Standard CI electrode with 12 contact pairs (MED-EL, Innsbruck, Austria) was inserted through the round window into scala tympani. Finally, the high-resolution model of the cochlea was embedded in a segmented human head model, which was derived from an MRI scan with 1 mm resolution. The current-controlled stimulation scheme was monopolar with an electric current of 1 mA per electrode contact pair. The reference electrode with a radius of approximately 1 cm was placed extracochlearly on the left temporal bone of the skull.

All surface meshes were then transferred to ANSYS ICEM CFD (ANSYS, PA, USA) and a tetrahedral volumetric mesh was generated with appropriate meshing and coarsening parameters. The volumetric mesh with 21,937,778 elements was exported to COMSOL Multiphysics (COMSOL AB, Sweden), conductivity values [4] were assigned and then the current spread inside the cochlea and the head was computed.

Nerve action potentials were calculated using multi-compartment models of all 400 reconstructed SGNs and with different degeneration states (see Figure 1). The models comprised of dendrite, soma and axon. In the dendrites and axons electrically active nodes of Ranvier were separated by insulating myelinated compartments. The soma was only partly myelinated and contained electrical excitable ion channels [5]. Axon diameter was $4 \mu\text{m}$. Three degeneration states were simulated for the entire population: SGNs with complete dendrites ($2 \mu\text{m}$ diameter), partly degenerated SGNs, where the dendrite diameter shrunk to $0.5 \mu\text{m}$ and fully degenerated SGNs with no more dendrite. SGNs were stimulated with biphasic pulses ($40 \mu\text{s}$ phase duration), cathodic phase first. Electrical stimulation was driven by the extracellular potentials at the nodes of Ranvier, which was derived from the finite element model. Firing thresholds (THR) were determined by iteration with a bisection algorithm.

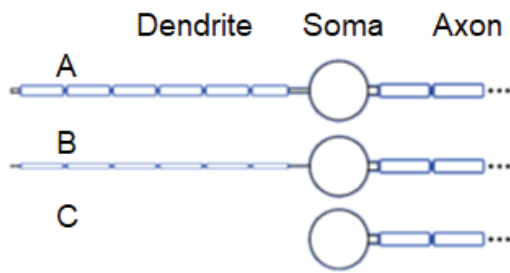


Figure 1: Morphologies of the SGN models based on [6]. All dendrites and axons were myelinated, denoted by the blue color. A: SGN with full dendrite (2 μm diameter); B: partly degenerated SGN with thin dendrite; C: SGN with completely degenerated dendrite. Figure is not to scale.

Results

Figure 2 shows excitation patterns for the 400 modeled SGNs. While in general the lowest thresholds were reached for neurons, which were closest to the electrode position, excitation patterns were very broad. While the excitation centroid moved from basal to apical with increasing electrode numbers, excitation patterns were rough, which reflects the irregular geometry of the nerve compartment inside the modiolus. Cross-turn stimulation (marked with blue arrows) caused multiple peaks. The excitation site of the action potentials (APs) is color coded in Figure 2. It was usually located at the dendrite and shifted centrally for higher stimulation levels. When the dendrite was absent, most APs were elicited at the soma.

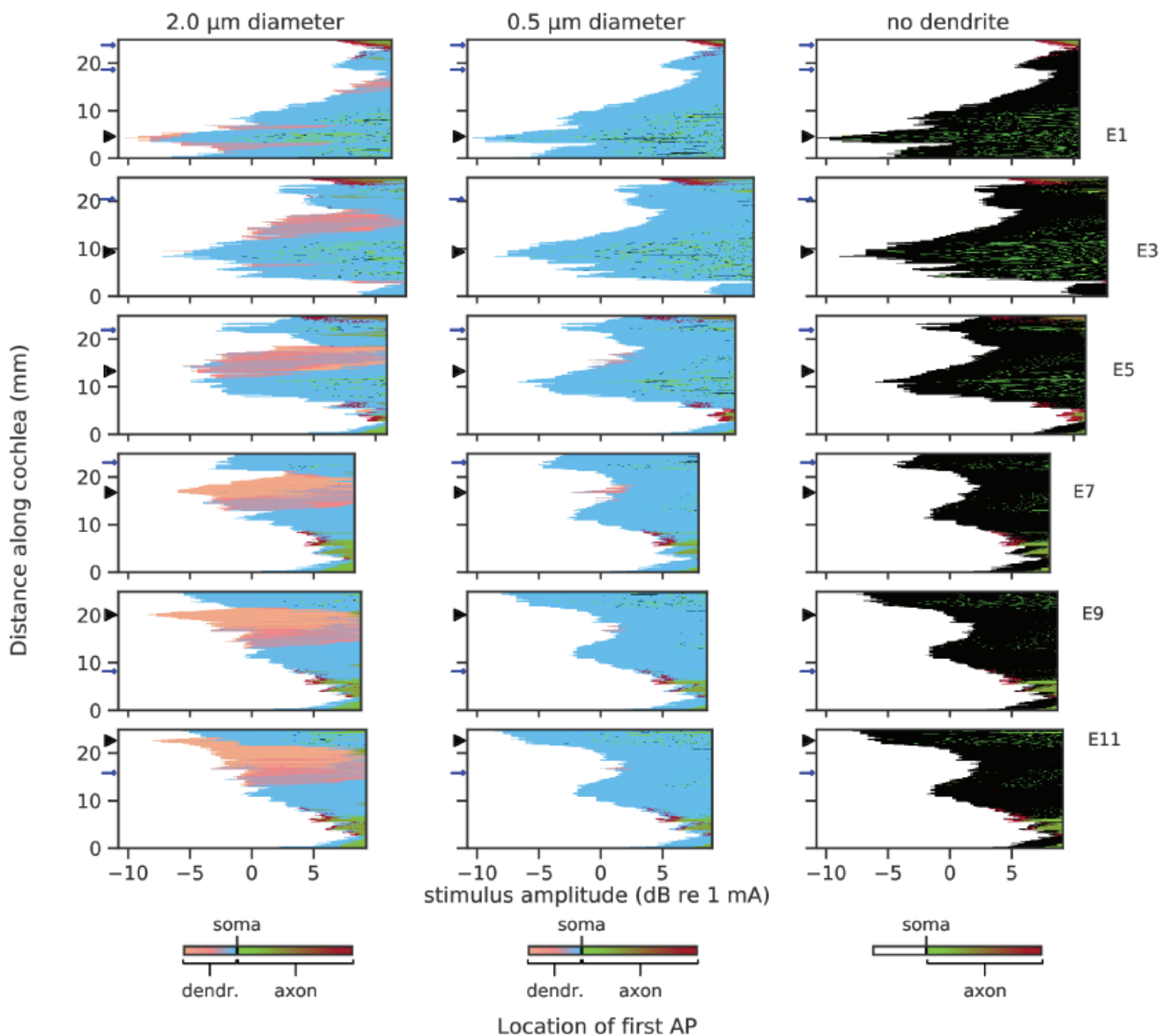


Figure 2: Comparison of neuronal activation patterns for SGNs with different degeneration states. Left column: SGNs with 2 μm diameter dendrite. Mid column: partly degenerated SGN with thin dendrite (0.5 μm diameter). Right column: SGNs with completely degenerated dendrite. The color map marks the location of the last independent AP along the ANFs. Black color denotes that APs originated from the soma. Each row depicts the responses for a stimulating electrode, position marked by the black triangle on the ordinates, with E1 being the most basal one and E12 the most apical. Cross-turn stimulation ($\pm 360^\circ$ relative to stimulation electrode position) is marked by blue arrows.

For ITD coding, the AP latencies are essential, data for six selected SGNs are displayed in detail in Figure 3 (stimulation with the most apical electrode E12). SGNs with intact dendrites showed long latencies and the large delay of the APs elicited in the dendrite by the soma can be observed. This delay (~ 5 ms) was overcome at stimulation levels of about 5 dB above THR. Latencies were longer for APs initiated near the peripheral terminal of the dendrite and they decreased monotonically with increasing stimulation current. Different neurons exhibited very different latency contours. For partly degenerated SGNs with thin dendrite, APs initiated near the peripheral terminal show consistently highest latencies (data not shown). This was completely different when the dendrites were completely degenerated. Latencies were much shorter and they only increased for stimulation levels close to their individual THRs.

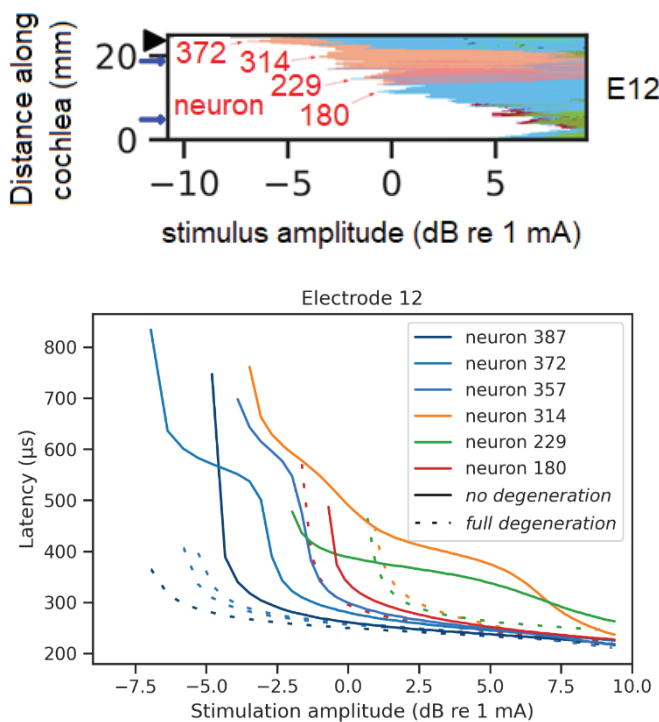


Figure 3: Upper panel: Neuronal activation pattern of SGNs for stimulation with the most apical electrode (E12, position marked with a black triangle, compare Figure 2). Lower panel: Latency plots of marked SGNs. Latency was defined as the time in between the stimulus onset and an AP arriving at a compartment at the measuring point, at 5.8 mm along the neuron measured from the peripheral terminal.

Figure 4 shows latency histograms (50 μ s time bins) for different stimulation currents. Levels were chosen such that about 10% (“soft”) 25% (“medium”) and 40% (“loud”) of the fiber population was excited (please note that this scaling is somehow arbitrary, as in humans the loudness growth function is not accessible). We only considered SGNs with characteristic frequencies below 1.5 kHz, because only these neurons contribute to ITD extraction in the medial superior olive (MSO) [7]. In the non-degenerated case, the latency spread was largest with 550 μ s (250 – 800 μ s) for the medium stimulation level and still 300 μ s (250 – 550 μ s) for high levels. In addition, latencies showed a distribution with two

peaks. With a degenerated dendrite, when APs were elicited at the soma, latencies were shorter and most of them were within a small range of about 100 μ s.

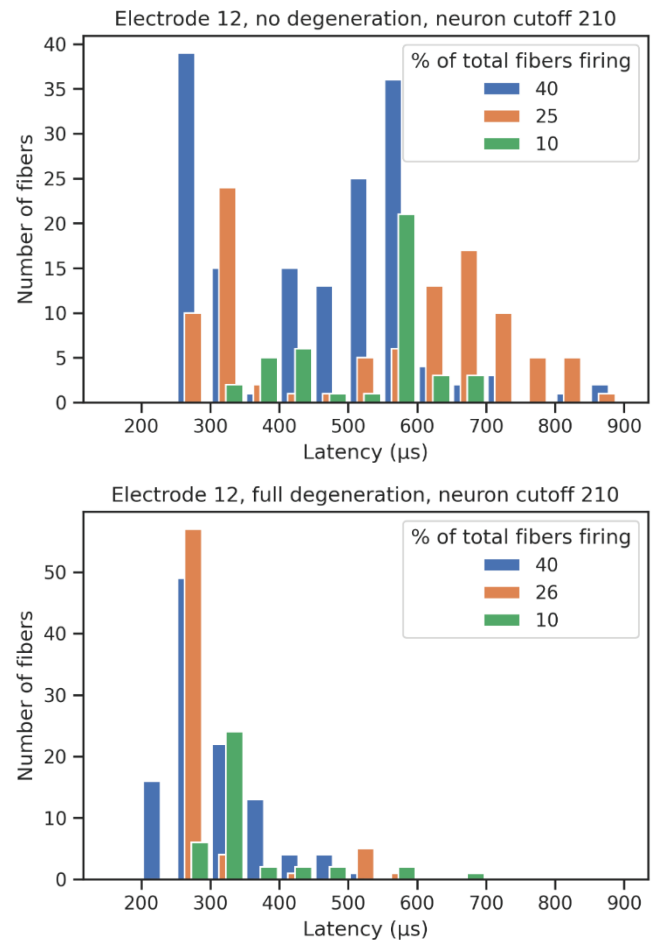


Figure 4: Latency histograms for three stimulation levels, which excited about 10%, 25% and 40% of the SGN population. Stimulation with E12 (most apical electrode). Upper panel: SGNs with intact dendrites. Lower panel: SGNs with fully degenerated dendrite. Only low-frequency SGNs with characteristic frequencies below 1.5 kHz (neurons 210-400) were selected.

Conclusion

We have developed a morphologically accurate model of the human inner ear based on high-resolution μ CT scans, which allowed us to reconstruct the path of SGNs and to calculate the current spread in the inner ear. With this data, we derived excitation patterns for 400 biophysically motivated multi-compartment SGN models with Hodgkin-Huxley type ion channels. We considered degeneration of SGNs by a shrinking diameter of their dendrites and its complete loss.

Our model provides many quantitative insights how a population of SGNs is excited by electrical stimulation. We skip a more detailed discussion here and focus on the analysis of spike time latencies due to their importance for ITD extraction in the MSO. Nerve fiber recordings in cat have previously revealed highly synchronized responses to electrical stimulation [3], but also that spike latencies

decreased with stimulation level in individual fibers. Our population model allows to analyze and compare many SGNs along the cochlea, which is very hard to achieve in physiological recordings. We found that spike latencies in a population covered a relatively large range of up to 500 μs , but only if their dendrites were present. As soon as SGNs have lost their dendrites, as it is probably the case in most long-term deaf CI users, APs were almost always elicited at the soma and spike latencies were within a range of only 100 μs (which is also the range for spike jitter [3]). Now the question arises, why these highly synchronized and sharper than normal excitation patterns can no longer be processed by the MSO? To understand what happens, we have to analyze the function of the MSO circuit. MSO processing relies on a delicate balance between excitation and inhibition from both left and right ear. When we look at neuronal coding in the intact hearing system, we can observe that the fine structure of the neuronal excitation patterns of SGNs [8] follow the stimulation frequency, as long as phase locking is present. The temporal shape of the firing patterns is therefore dominated by the sinusoidal stimulus, its width scales inversely with stimulus frequency (compare Figure 5, grey lines). If the MSO would act as a simple coincidence detector, coincident inputs from left and right ear would cause maximal excitation. Now we consider inhibition, which is also sinusoidal shaped and subtracted from the excitation to the MSO neurons. As the inhibitory inputs to the MSO have longer time constants, it gets delayed. When excitation and inhibition are combined, the total MSO excitation also has a sinusoidal shape, but gets shifted by about a quarter of a period (different directions left and right) in the healthy hearing system (compare Figure 5, grey lines). This condition is optimal for an opponent-channel ITD decoder, left and right MSOs convert the time critical ITD code into a robust rate code. It has to be noted that this mechanism requires that excitatory and inhibitory inputs and their time constants are precisely adjusted.

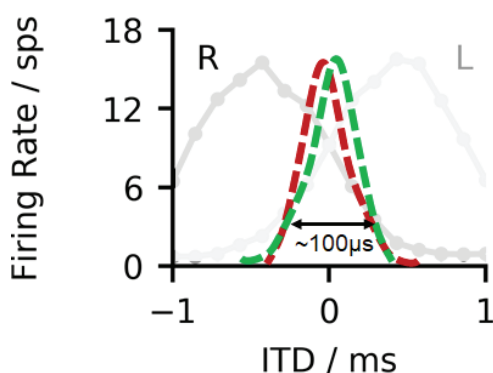


Figure 5: Schematic model of MSO activity in the left and right hemisphere for the intact inner ear (grey lines, marked with R/L). For over-synchronized electrical stimulation (red and green lines) the activity of left and right MSO is almost identical, therefore ITD decoding breaks down.

However, the shift mechanism only works for sinusoidal modulated excitation patterns. If we now consider over-synchronized excitation patterns, an inhibition mechanism (unlike a delay-line mechanism) can alter excitation only while it is active. For the over-synchronized electrical responses, excitation lasts less than 100 μs . This is far less

than the shift required at frequencies below 1 kHz, where ITD decoding is most sensitive [7]. Also, excitation patterns from the left and right ear can only add up for coincidence detection in an MSO neuron when they overlap (compare Figure 5, red and green lines). For ITDs larger than the SGN latency distribution, there is no more MSO activity and ITD decoding is not possible. While this explanation provides a fundamental argument why ITD coding for electrical stimulation breaks down in the MSO even under optimal stimulus conditions, there might also be other reasons. For example, over-synchronized inputs from only one ear might already cause the MSO to fire, independent of the input of the other ear, if the balance between excitation and inhibition is not precisely re-adjusted. We would also argue that the reason why there is some reduced ITD sensitivity in CI users is due to the processing in the lateral superior olive (LSO). At the LSO, the subtraction of left and right inputs (and not coincidence detection) and its longer time constants would work even for over-synchronized inputs, albeit less precise.

Acknowledgements

This study was funded by the Deutsche Forschungsgemeinschaft (DFG, German Research Foundation) – project number: 415658392.

References

- [1] Nicoletti, M., Wirtz, C., Hemmert, W.: Modeling sound localization with cochlear implants. In: Blauert, J. (ed.) *The technology of binaural listening*. ASA press & Springer, Berlin, Heidelberg (2013), 309-331.
- [2] Laback, B., and Majdak, P.: Binaural jitter improves interaural-time difference sensitivity of cochlear implantees at high pulse rates. *Proc. Natl. Acad. Sci. U.S.A.* **105** (2008), 814–817.
- [3] Shepherd, R.K., and Javel, E.: Electrical stimulation of the auditory nerve. I. Correlation of physiological responses with cochlear status. *Hearing research* 108.1-2 (1997): 112-144.
- [4] Bai, S., Encke, J., Obando-Leitón, M., Weiß, R., et al.: Electrical stimulation in the human cochlea: A computational study based on high-resolution micro-CT scans. *Frontiers in Neuroscience*, 13 (2019): 1312.
- [5] Bachmaier, R., Encke, J., Obando-Leitón, M., Hemmert, W., Bai, S.: Comparison of multi-compartment cable models of human auditory nerve fibers. *Frontiers in Neuroscience*, 13 (2019): 1173.
- [6] Rattay, F., Potrusil, T., Wenger, C., Wise, A. K., Glueckert, R., and Schrott-Fischer, A.: Impact of morphometry, myelination and synaptic current strength on spike conduction in human and cat spiral ganglion neurons. *PLoS ONE* 8 (2013): e79256
- [7] Brughera, A., Dunai L., Hartmann, W.M.: Human interaural time difference thresholds for sine tones: The high-frequency limit. *JASA* 133.5 (2013): 2839-2855.
- [8] Encke, J., Hemmert, W.: Extraction of inter-aural time differences using a spiking neuron network model of the medial superior olive. *Frontiers Neurosc*, 12 (2018):140.